DÉPARTEMENT DE GÉNIE ÉLECTRIQUE
SECTION AUTOMATIQUE

ON THE MOTION CONTROL OF ELECTRIC AGVS

par

Romano M. DeSantis, Richard Hurteau

EPM/RT-89/22

Dépôt légal, 3e trimestre 1989
Bibliothèque nationale du Québec
Bibliothèque nationale du Canada

Pour ce procurer une copie de ce document, s'adresser au:

Editions de l'Ecole Polytechnique de Montréal
Ecole Polytechnique de Montréal
Case postale 6079, Succursale A
Montréal (Québec) H3C 3A7
(514) 340-4000

Compter 0,10$ par page (arrondir au dollar le plus près) et ajouter 3,00$ (Canada) pour la couverture, les frais de poste et la manutention. Régler en dollars canadiens par chèque ou mandat-poste au nom de l'Ecole Polytechnique de Montréal. Nous n'honorerons que les commandes accompagnées d'un paiement, sauf s'il y a eu entente préalable dans le cas d'établissements d'enseignement, de sociétés ou d'organismes canandiens.

EPM/RT-89/22

ON THE MOTION CONTROL OF ELECTRIC AGVS

par

Romano M. DeSantis, Richard Hurteau

DÉPARTEMENT DE GÉNIE ÉLECTRIQUE

ÉCOLE POLYTECHNIQUE DE MONTRÉAL

NOVEMBRE 1989

ON THE MOTION CONTROL OF ELECTRIC AGVS

Romano M. DeSantis, Richard Hurteau
Ecole Polytechnique de Montréal
P.O. Box 6079 - Station "A"
Montréal, Canada
H3C 3A7

0.Abstract

A simple and effective procedure for the design of advanced motion controllers for electric powered AGVs is presented which incorporates many of the ideas characterizing the recently established theory on the control of robotic manipulators. This includes dynamic modelling, decoupling, pre-computed torque, linearization, pole placement and sliding modes. Selected results from extensive simulation and field experiments illustrate its application and support its validity.

ON THE MOTION CONTROL OF ELECTRIC AGVS

Romano M. DeSantis, Richard Hurteau
Ecole Polytechnique de Montréal
P.O. Box 6079 - Station "A"
Montréal, Canada
H3C 3A7

TABLE OF CONTENTS

List of symbols

L	Distance between the drive wheels
R_{a1}, R_{a2}	Drive wheel radius
f_1, f_2	Drive wheel viscous damping coefficient
V_1, V_2	Voltage applied to the servo-motors
Γ_1, Γ_2	Torque applied by the servo-motor on the drive wheel axle
F_1, F_2	Force applied to the drive wheel
$PERT_1$, $PERT_2$	Perturbation applied to the drive wheel
R_{e1}, R_{e2}	Servomotor internal resistance
K_{b1}, K_{b2}	Servomotor Voltage constant
$K_{\Phi 1}$, $K_{\Phi 2}$	Servomotor Torque constant
M	Mass of the Vehicle
J	Moment of Inertia of the Vehicle w/r to its z axis
θ_1, θ_2	Angular Position of the drive wheel
x_c, Y_c	Vehicle frame origin coordinates w/r to a fixed frame
SPEED	Vehicle translation speed
Φ, ORIENT	Vehicle orientation
A, B, B	Matrices of the (nonlinear) state model
LAT_OFFSET	Vehicle lateral offset
ORIENT_OFFSET	Vehicle orientation offset
$u_M = (V_1+V_2)/2$	Speed controller action
$\Delta u = (V_2-V_1)/2$	Position/orientation controller action
K_{SPEED}, τ_{SPEED}	Vehicle speed gain and time constant
K_{ORIENT}, τ_{ORIENT}	Vehicle orientation gain and time constant
ξ_1, ξ_2	Input equivalent perturbation
K_{ij}	Motion Controller Linear Component Gains
a_{ij}, M_i, ϵ_i, ξ_i	Motion Controller Switching Component Parameters

List of figures

1. Introduction

The development of guidance systems for automatically guided vehicles (AGVs) operating in an only partially structured environment (such as that found in office, hospital and a number of industrial applications) requires the solution of a number of basic problems: environmental perception, world modelling, trajectory planning, motion control, etc.. [7, 8, 17, 18]. Among these, motion control, the problem of generating the propulsion forces required for the vehicle dynamics to conform to the desired trajectory, while certainly not the most difficult, is nevertheless the one with which the designer is most often confronted.

In spite of this fact, and aside from a few exceptions [12, 13, 18], the technical literature appears to have paid only a scant attention to the development of design procedures for AGVs motion controllers. Apparently, the problem has either been seen as a simple corollary of the larger problem of motion control for a general robotic manipulator [17], and as such not worthy of a specialized treatment, or, it has been considered as implicitely embedded in the more complex motion control of autonomous vehicles for automotive applications [4-6]. These latter developments, however, are so cluttered with such complex aspects as high speed dynamic modelling, tire deformation and spring effects, roll and pitch oscillations as to appear of a moderate relevance to the design of motion controllers for low speed, 2-D AGVs where the emphasis is rather on accuracy, repeatability and robustness to changing operating conditions.

As a contribution to improve this situation, in what follows we present a systematic procedure for the design of advanced motion controllers for industrial AGVs which we have established in the course of research on the development of AGVs for the automatisation of mining operations [3]. The class of AGVs considered is of the type which are propelled by a locomotion module equipped with two front castors and two rear co-axial drive wheels; each of the drive wheels is independently powered by a DC servomotor which is in turn energized by a PWM amplifier (figures 1, 2). The approach, based on theoretical analysis, simulation and field experiments, is somewhat similar in spirit to [12] where the same class of AGVs is considered. Among its innovative features, (with respect to [12]), one may mention: the development of a more general plant model incorporating the interactions between servomotor and vehicle dynamics; the study of a more comprehensive motion controller simultaneously concerned with speed lateral and orientation control; a more general design procedure easily adaptable to other classes of AGVs, including AGVs with a steering wheel.

The main steps of the development are the classical ones [1]: the attainment of the vehicle dynamic model, the linearization of this model, the application of the computed torque method, the exploitation of classical decoupling and pole placement techniques [9], the potential incorporation of more advanced control features (sliding mode) [10, 11].

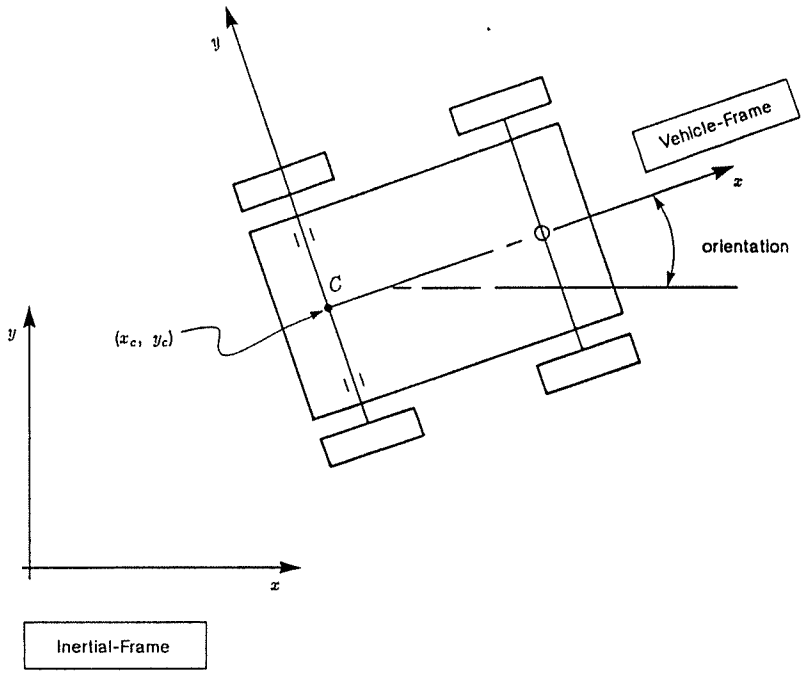

Figure 1: Locomotion module geometry

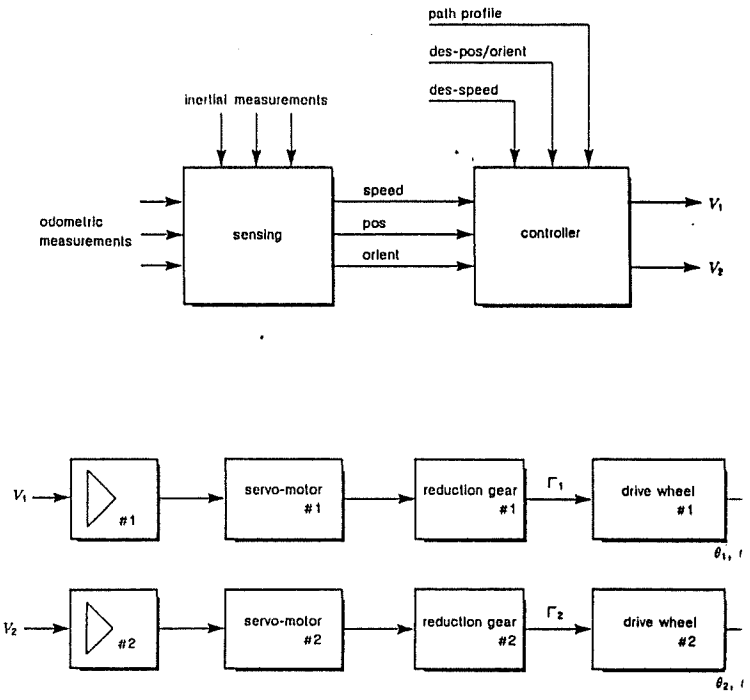

Figure 2: Motion controller elements

2. The vehicle dynamic model

The vehicle dynamic model has the function to compute speed, position and orientation as influenced by the voltages applied to the locomotion module servomotors. For the class of AGVs under consideration a useful yet quite applicable simplification is obtained by neglecting such aspects as vehicle roll and pitch dynamics, vehicle and drive wheels slippage, deformation and spring effect in the tires (all elements which must instead be considered in the more complex automotive vehicles case [4-6]).

With this simplification, the position and orientation of the vehicle may be described in terms of the angular position of the drive wheels according to the following equations

$$\dot{ORIENT} = \frac{R_{a2}\,\dot{\theta}_2 - R_{a1}\,\dot{\theta}_1}{L}$$

$$\dot{x}_c = \frac{R_{a2}\,\dot{\theta}_2 + R_{a1}\,\dot{\theta}_1}{2} \cos(ORIENT)$$

$$\dot{y}_c = \frac{R_{a2}\,\dot{\theta}_2 + R_{a1}\,\dot{\theta}_1}{2} \sin(ORIENT)$$

where (x_c, y_c) are the coordinates of the origin of a frame attached to the vehicle with respect to a fixed frame; ORIENT is the angle characterizing the orientation of the vehicle frame with respect to the fixed frame; θ_1, θ_2 represent the angular position of the drive wheels; R_{a1}, R_{a2} denote the drive wheels radius; L is the distance between the drive wheels.

The dynamic evolution of the angular position of the drive wheels as a function of the voltages applied to the servomotors, may be obtained by combining the Newton equations [1]

$$F_1 + F_2 = \frac{M}{2} (R_{a2} \ddot{\theta}_2 + R_{a1} \ddot{\theta}_1)$$

$$(F_2 - F_1)\frac{L}{2} = J(R_{a2} \ddot{\theta}_2 - R_{a1} \ddot{\theta}_1)$$

with the servomotor dynamic equations [14]

$$\Gamma_i = \frac{V_i - K_{bi} \dot{\theta}_i}{R_{ei}} K\Phi_i - f_i \dot{\theta}_i$$

where

$$F_i = \frac{\Gamma_i}{R_{ai}} - PERT_i$$

The symbols F_1, F_2 denote the equivalent propulsion forces applied to the drive wheels; Γ_1, Γ_2 the torques applied by the servo-motors to the drive wheels; $PERT_1$, $PERT_2$ the equivalent perturbation forces acting on the drive wheels; M the mass of the vehicle; J the moment of inertia of the vehicle with respect to its yaw axis; f_1, f_2 the drive wheel viscous damping coefficients; V_1, V_2 the voltages applied to the inductor of the servo-motors; R_{e1}, R_{e2} the internal resistances of the servo-motors; K_{b1}, K_{b2} the servomotor voltage constants; $K_{\Phi1}$, $K_{\Phi2}$ the servomotor torque constants.

It follows

$$\ddot{\theta}_1 = -\left[\left(\frac{L^2}{4J} + \frac{1}{M}\right) \left(f_1 + \frac{K_{b1} K_{\Phi 1}}{R_{e1}}\right) \frac{1}{R_{a1}^2} \right] \dot{\theta}_1$$

$$+\left[\left(\frac{L^2}{4J} - \frac{1}{M}\right) \left(f_2 + \frac{K_{b2} K_{\Phi 2}}{R_{e2}}\right) \frac{1}{R_{a1} R_{a2}} \right] \dot{\theta}_2$$

$$+\left[\left(\frac{L^2}{4J} + \frac{1}{M}\right) \frac{K_{\Phi 1}}{R_{e1} R_{a1}^2} \right] V_1$$

$$+\left[\left(\frac{1}{M} - \frac{L^2}{4J}\right) \frac{K_{\Phi 2}}{R_{e2} R_{a1} R_{a2}} \right] V_2$$

$$-\left[\frac{L^2}{4J} + \frac{1}{M} \right] \frac{PERT_1}{R_{a1}}$$

$$-\left[\frac{1}{M} - \frac{L^2}{4J} \right] \frac{PERT_2}{R_{a1}}$$

$$\ddot{\theta}_2 = \left[\left(\frac{L^2}{4J} - \frac{1}{M}\right) \left(f_1 + \frac{K_{b1} K_{\Phi 1}}{R_{e1}}\right) \frac{1}{R_{a1} R_{a2}} \right] \dot{\theta}_1$$

$$-\left[\left(\frac{L^2}{4J} + \frac{1}{M}\right) \left(f_2 + \frac{K_{b2} K_{\Phi 2}}{R_{e2}}\right) \frac{1}{R_{a2}^2} \right] \dot{\theta}_2$$

$$+\left[\left(\frac{1}{M} - \frac{L^2}{4J}\right) \frac{K_{\Phi 1}}{R_{e1} R_{a1} R_{a2}} \right] V_1$$

$$+\left[\left(\frac{1}{M} + \frac{L^2}{4J}\right) \frac{K_{\Phi 2}}{R_{e2} R_{a2}^2} \right] V_2$$

$$-\left[\frac{1}{M} - \frac{L^2}{4J} \right] \frac{PERT_1}{R_{a2}}$$

$$-\left[\frac{1}{M} + \frac{L^2}{4J} \right] \frac{PERT_2}{R_{a2}}$$

While these equations are essential for simulation purposes, a more convenient for design purposes state space model may be obtained from them by choosing as the state vector

$$x' \triangleq [\ \text{SPEED ORIENT } \dot{\text{ORIENT}}\ x_c\ y_c\ ]$$

and as the control vector

$$u' \triangleq [\ u_M \qquad \Delta u\ ]$$

where

$$u_M \triangleq \frac{V_1 + V_2}{2}$$

$$\Delta u \triangleq \frac{V_2 - V_1}{2}$$

$$\text{SPEED} \triangleq \frac{R_{a2}\,\dot{\theta}_2 + R_{a1}\,\dot{\theta}_1}{2}$$

With this choice of state and control vectors one has

$$\dot{x} = Ax + Bu + B'\xi$$

where

$$A \triangleq \begin{bmatrix} a_{11} & 0 & 0 & 0 & 0 \\ 0 & 0 & 1 & 0 & 0 \\ 0 & a_{32} & 0 & 0 & 0 \\ a_{41} & 0 & 0 & 0 & 0 \\ a_{51} & 0 & 0 & 0 & 0 \end{bmatrix}$$

$$B \triangleq \begin{bmatrix} b_{11} & 0 \\ 0 & 0 \\ 0 & b_{32} \\ 0 & 0 \\ 0 & 0 \end{bmatrix} \qquad B' \triangleq B$$

and

$$a_{11} \triangleq -1/\tau_{SPEED} \qquad a_{32} \triangleq -1/\tau_{ORIENT}$$

$$a_{41} \triangleq \sin(ORIENT) \qquad a_{51} \triangleq \cos(ORIENT)$$

$$b_{11} \triangleq K_{SPEED}/\tau_{SPEED}$$

$$b_{32} \triangleq K_{ORIENT}/\tau_{ORIENT}$$

$$\tau_{SPEED} \triangleq \left[\frac{2}{MR_a^2} \left(f + \frac{K_b K\Phi}{R_e} \right) \right]^{-1}$$

$$K_{SPEED} \triangleq \frac{R_a}{K_b \left(1 + f \dfrac{R_e}{K_b K\Phi}\right)}$$

$$\tau_{ORIENT} \triangleq \left[\frac{2L^2}{4J R_a^2} \left(f + \frac{K_b K\Phi}{R_e} \right) \right]^{-1}$$

$$K_{ORIENT} \triangleq \frac{2R_a/L}{K_b \left(1 + f \dfrac{R_e}{K_b K\Phi}\right)}$$

The symbol $\xi \triangleq [\xi_1 \ \xi_2]$ represents an equivalent perturbation which takes into account the influence of PERT, plus the potential lack of symmetry between left and right side vehicle parameters.

Remark 1. In the special case where $M=4J/L^2$ this model coincides with that proposed in [12].

Remark 2. In view of unaccounted for viscous damping in the castors, in practical applications K_{ORIENT} will be smaller than $(2/L)K_{SPEED}$.

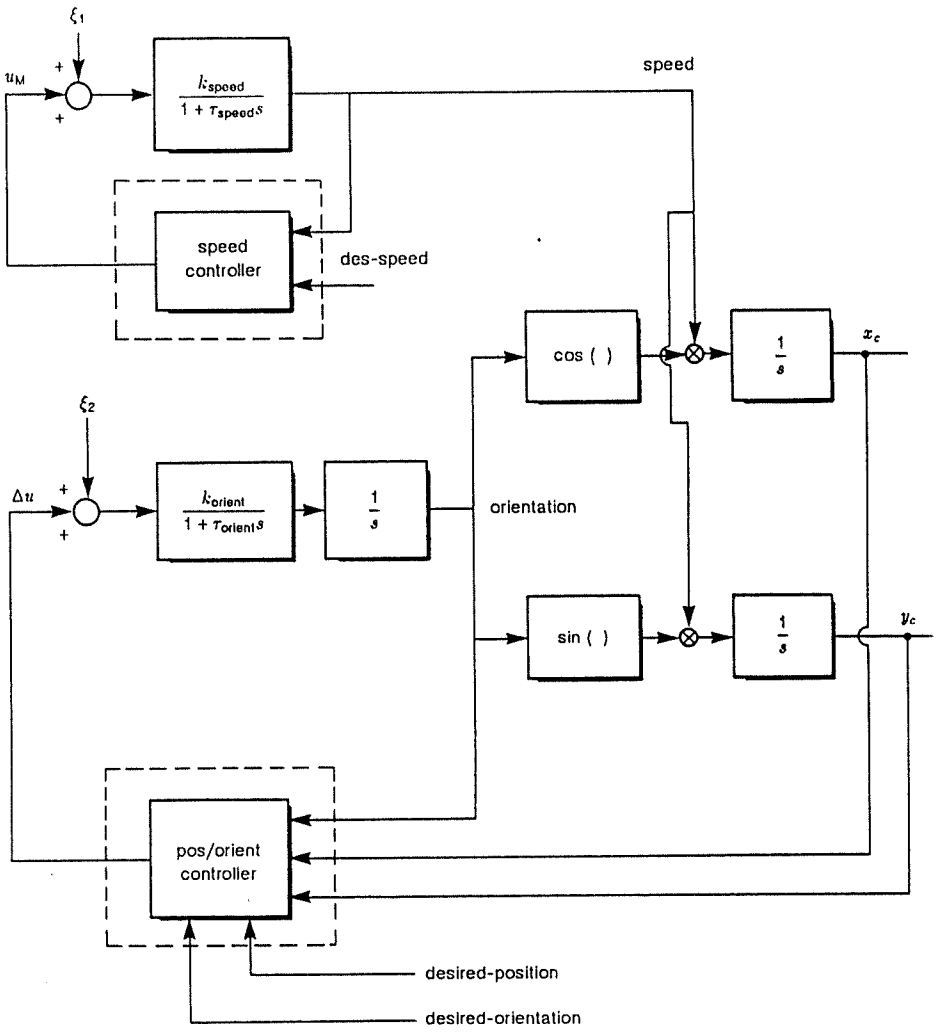

Figure 3: Vehicle simplified model and motion controller structure

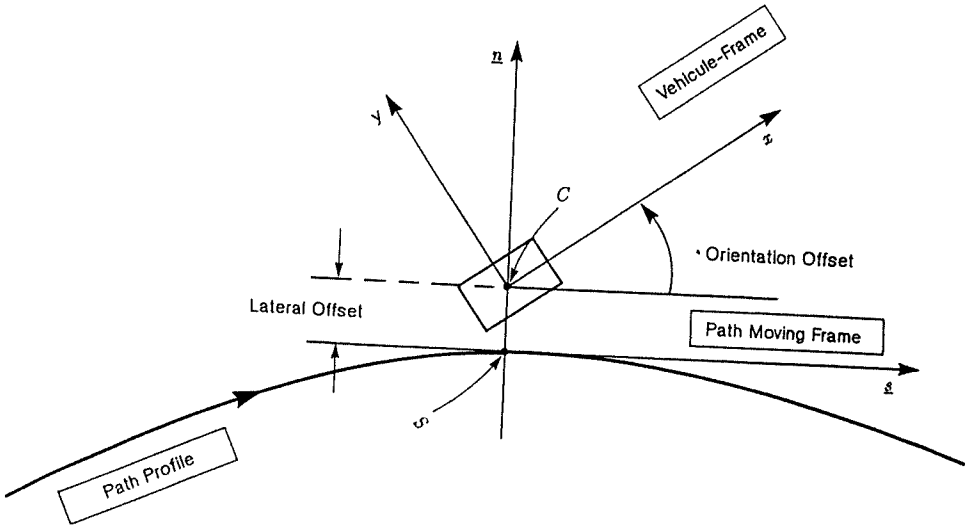

Figure 4: Lateral and orientation offsets

3. Motion controller design

From the available estimate of speed, position and orientation of the vehicle, the motion controller has the task of computing the control voltages required to have the vehicle follow a given path with a prescribed value of these parameters (possibly a function of actual speed and position of the vehicle with respect to the path). This computation is implemented by considering the concepts of lateral and orientation offsets which are defined as follows. Denote with S the point of the path which is closest to the actual position of C, the origin of the vehicle reference frame; consider a path dependent frame with origin in S, x axis tangent to the path and pointing in the direction of the desired motion, z axis vertical and opposite to gravity. The lateral offset of the vehicle with respect to the path, LAT_OFFSET, is the (signed) distance between C and S; the orientation offset, ORIENT_OFFSET, is the orientation of the vehicle frame with respect to the path dependent frame.

The lateral offset of the vehicle corresponds to the y coordinate of the origin of the vehicle frame with respect to the path dependent frame that is

$$\text{LAT\_OFFSET} = n_1 \; x_c + n_2 \; y_c$$

where $\underline{n} = (n_1, n_2)$ is the unit vector perpendicular to the path at S (see figure 4). The orientation offset is given by

$$\text{ORIENT\_OFFSET} \triangleq \text{DES\_ORIENT} - \text{ORIENT}$$

where DES_ORIENT is the orientation of the path dependent frame at S.

Usage of these concepts together with the decoupled form of the vehicle state space model obtained in the previous section, suggest that the motion controller be viewed as given by the ensemble of two decentralized control loops:

- a translational speed controller loop to generate the control action u_M required to reduce to zero the difference between actual and desired translational speed of the vehicle;
- a position/orientation controller loop to generate the control action Δu required to reduce to zero the lateral and the orientation offset of the vehicle.

In line with the precomputed torque approach [1], the control u_M generated by the traslational speed controller is chosen as given by the contribution of two components

$$u_M = u_{M1} + u_{M2}$$

where:

u_{M1} : is a feedforward component corresponding to the control action required to obtain the desired speed under nominal conditions and in the absence of perturbations;

u_{M2} : is a linear PI feedback component with the task of reducing the influence of parameter variations, external disturbances and model uncertainties.

These components are computed via the following formulas

$$u_{M1} = \frac{\tau_{SPEED}}{K_{SPEED}} \dot{DES\_SPEED} + \frac{1}{K_{SPEED}} DES\_SPEED$$

$$u_{M2} = K_{11} * SPEED\_OFFSET + K_{12} \int SPEED\_OFFSET \, dt$$

where

$$SPEED\_OFFSET \triangleq DES\_SPEED - SPEED$$

The symbol DES_SPEED represents the desired translational speed; K_{11}, K_{12} are the controllers gains.

The value of these gains is determined by imposing that the dynamics of the speed offset be described by pre-assigned poles p_{11} and p_{12}; this gives

$$K_{11} = - \left(\frac{p_{11} + p_{12}}{\tau_{SPEED}} + 1 \right) / K_{SPEED}$$

$$K_{12} = p_{11} \, p_{12} \, \tau_{SPEED} / K_{SPEED}$$

To design the position/orientation controller, it is useful to note that under tight control conditions, (i.e. under small speed and orientation offsets), one can use the following linear approximations

$$SPEED \check{=} DES\_SPEED$$

$$\sin(ORIENT\_OFFSET) \tilde{=} ORIENT\_OFFSET$$

$$\cos(ORIENT\_OFFSET) \check{=} 1$$

and obtain

$$\dot{ORIENT\_OFFSET} = - \frac{1}{\tau_{ORIENT}} ORIENT\_OFFSET + \frac{K_{ORIENT}}{\tau_{ORIENT}} (\Delta u + \xi_2)$$

$$\dot{LAT\_OFFSET} = DES\_SPEED * ORIENT\_OFFSET$$

In analogy with the translational speed controller, one may then once again apply the pre-computed torque idea and view the control action Δu as given by the contribution of

Δu_1 : a feed_foward component corresponding to the control action required to obtain the desired orientation under nominal conditions and in the absence of perturbations;

Δu_2 : a PID feedback component with the task of reducing the influence of parameter variations, external disturbances and model uncertainties.

These components are computed by

$$\Delta u_1 = \tau_{ORIENT} \frac{DES\_\ddot{O}RIENT}{K_{ORIENT}} + \frac{DES\_\dot{O}RIENT}{K_{ORIENT}}$$

$$\Delta u_2 = K_{21}\ ORIENT\_OFFSET + K_{22}\ \dot{ORIENT}\_OFFSET + \frac{K_{23}}{DES\_SPEED} LAT\_OFFSET$$

where K_{21}, K_{22}, and K_{23} are the controller's gains.

The value of these gains is determined by imposing that the dynamics of position and orientation offsets be described in terms of pre-assigned poles p_{21}, p_{22} and p_{23}. This leads to

$$K_{21} = (p_{21}\ p_{22} + p_{21}\ p_{23} + p_{22}\ p_{23})\ \tau_{ORIENT} / K_{ORIENT}$$

$$K_{22} = -((p_{21} + p_{22} + p_{23})\ \tau_{ORIENT} + 1)/K_{ORIENT}$$

$$K_{23} = -\ p_{21}\ p_{22}\ p_{23}\ \tau_{ORIENT}/K_{ORIENT}$$

4. A sliding mode motion controller

Under most operating conditions the usage of the above motion controller is characterized by a satisfactory dynamic behavior and an adequate steady state disturbance rejection. In exceptional situations, however, the presence of large variations in operating conditions, model nonlinearities, and excessive external perturbations (e.g.: static friction) may on occasion lead to unpredictable, out of specification behavior. One way to overcome this difficulty is to apply "ad hoc" nonlinear modifications such as the complementing of the linear actions with supplementary signals, the application of optimal and adaptive control, or the changing of the controller configuration as a function of the state of operation of the vehicle. With this approach, however, one is never quite sure about just what kind of modification will do.

As an alternative approach, one may reinforce the action of the linear motion controller by incorporating into it sliding mode features. As suggested in [10, 11], this may be done by simply adding to the original controller appropriately "fired" switching elements according to the schemes in figures 5 and 6. With this addition, the control action generated by the (PI/slm) translational speed controller may now be viewed as given by the contribution of three components

$$u_M = u_{M1} + u_{M2} + u_{M3}$$

where: u_{M1} and u_{M2} are identical to the components provided by the original controller discussed in the previous section; u_{M3} is an on/off feedback component which reinforces the intended effect of u_{M1} and u_{M2} by neutralizing the influence of parameter variations, external perturbations and model uncertainties.

By specifying that the vehicle follow the desired translational speed trajectory according to an error dynamics described by:

$$\text{SPEED\_OFFSET} + a_{11} * \dot{\text{SPEED\_OFFSET}} = 0$$

with

$$a_{11} = -1/p_{11}$$

the value of u_{M3} is computed via the formula

$$u_{M3} = M * \text{SIGN}[slm_1] \quad \text{if } |slm_1| > \epsilon_1, = 0 \text{ otherwise}$$

where

$$slm_1 \triangleq a_{11}\ \text{SPEED\_OFFSET} + \int \text{SPEED\_OFFSET}\ dt$$

and M_1 and ϵ_1 are additional controller parameters. Positive M_1 is chosen to be as large as possible up to the maximum expected value of the input equivalent perturbation ξ_1. Positive ϵ_1 is chosen so that under "small" speed offsets the controller feedback action coincides with that which would be provided by the original PI; under larger speed offsets, the more energetic action of the switching component comes into play.

Analogous considerations apply to the position/orientation controller. By specifying that the vehicle follow the assigned path with an error dynamics described by:

$$\frac{\text{LAT\_OFFSET}}{\text{DES\_SPEED}} + a_{21}\ \text{ORIENT\_OFFSET} + a_{22}\ \dot{\text{ORIENT}}\text{-OFFSET} = 0$$

with

$$a_{22} = 1/p_{21}p_{22} \qquad a_{21} = -a_{22}(p_{21} + p_{22})$$

the control action Δu may once again be viewed as given by

$$\Delta u = \Delta u_1 + \Delta u_2 + \Delta u_3$$

where: Δu_1 and Δu_2 are identical to the linear feedback component provided by the original PID controller; Δu_3 is a switching component with the objective of reinforcing the intended effect of Δu_1 and Δu_2. Δu_3 is computed by

$$u_3 \triangleq M_2\ \text{SIGN}\,[slm_2]\ \text{if}\ |slm_2| > \epsilon_2, = 0\ \text{otherwise}$$

where

$$slm_2 = \frac{\text{LAT\_OFFSET}}{\text{DES\_SPEED}} + a_{21}\ \text{ORIENT\_OFFSET} + a_{22}\ \dot{\text{ORIENT}}\text{-OFFSET}$$

and M_2 and ϵ_2 are additional controller parameters.

In analogy with the translational speed controller case, the value of positive M_2 is chosen so as to be as large as possible up to the maximum expected value of the input equivalent perturbation ξ_2. The value of positive ϵ_2 is chosen so that under "small" orientation and lateral offsets the controller feedback action coincides with that provided by a classical PID; under larger speed offsets, the more energetic action of the switching component comes to the rescue.

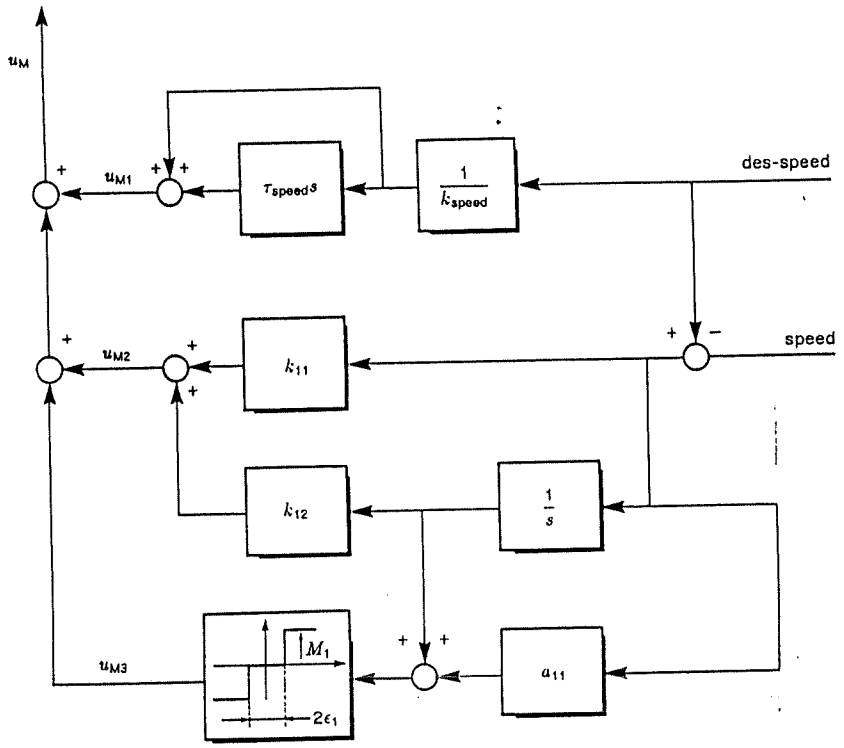

Figure 5: PI/slm translational speed controller

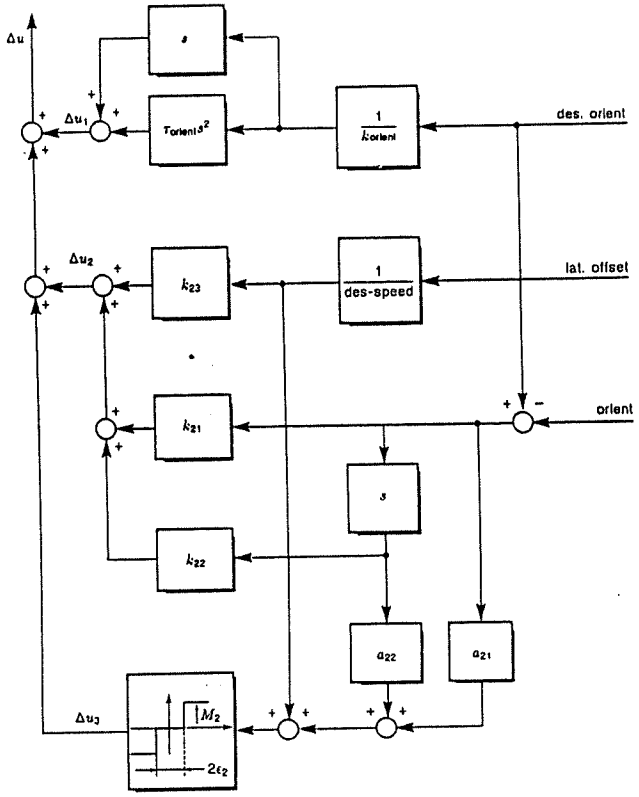

Figure 6: PID/slm position/orientation controller

5. An application example

To illustrate the above procedure we will apply it to the design of the motion controller presently installed in the AGV unit under development in our laboratory [3]. This unit uses the locomotion module of the power wheel chair model 6755 by Fortress Engineering Co. (a Montreal based company), which is characterized by precisely the same geometry, components, and dynamic model discussed in the previous sections.

Considering an operating mode where the vehicle has to follow a desired path with a pre-assigned speed and lateral offset and by taking into account the Fortress locomotion module parameter values reported in table 1, the motion controller will be characterized by the decentralized structure discussed in section 3. The gains of its components are calculated as follows.

Speed controller: By requiring $p_{11} = -3$ $p_{12} = -5$, one obtains

$$K_{11} = -[(p_{11} + p_{12}) * \tau_{SPEED} + 1]/K_{SPEED} = 5.7$$

$$K_{12} = p_{11}\, p_{12}\, \tau_{SPEED} / K_{SPEED} = 16.7$$

Position/orientation controller: By requiring $p_{21} = p_{22} = -1.5$ $p_{23} = -3$, one obtains

$$K_{21} = (p_{21}\, p_{22} + p_{21}\, p_{23} + p_{22}\, p_{23}) \frac{\tau_{ORIENT}}{K_{ORIENT}} = 6.2$$

$$K_{22} = -((p_{21} + p_{22} + p_{23})\, \tau_{ORIENT} + 1)/K_{ORIENT} = 2$$

$$K_{23} = -p_{21}\, p_{22}\, p_{23}\, \tau_{ORIENT}/K_{ORIENT} = 3.7$$

Distance between the drive wheels L = 0.5 m

Drive wheel radius $R_{a1} = R_{a2} = .12$ m

Mass of the Vehicle M = 200 Kg

Moment of Inertia of the Vehicle w/r to its yaw axis J = 12.5 Kg*m^2

Vehicle translational speed gain $K_{SPEED} = .32$ m/volt*sec

Vehicle translational time constant $\tau_{SPEED} = .35$ sec

Vehicle orientation gain $K_{ORIENT} = .8$ rad/volt*sec

Vehicle time constant $\tau_{ORIENT} = .5$ sec

Table 1: Fortress Locomotion Module (typical) Parameter Values

6. Simulation and test bench results

The dynamic behavior associated with the above design will be illustrated by discussing some selected results from a certain number of simulation and field experiments. For this we consider an implementation of the motion controller based on an IBM PC equipped with a LabMaster input/output interface; the vehicle speed and lateral and orientation offsets are computed from odometric measurements obtained by installing optical encoders on each drive wheel axis; the operator interface is provided by the PC keyboard. Though in the actual AGV unit currently under development in our laboratory a more refined position/orientation measuring system is used (via the addition of 2-D camera, a line painted on the ceiling, safety and guidance features), this simplified implementation is well sufficient for the intended purpose. The controller and encoders sampling periods used in

experiments 1, 2 and 3 are equal to 0.04 sec; the sampling periods in experiment 4 are equal to 0.005 sec.

Experiment N.1 (Simulation). This experiment illustrates the simulated response of the vehicle equipped with the above motion controller. The vehicle is requested to follow a straight line path with a constant speed equal to 5m/s. The initial conditions are characterized by a zero speed and various values of position and orientation offsets. Typical results are illustrated in figure 7. In agreement with a great number of other simulation tests [16], they illustrate that the motion controller should perform quite well under a variety of transient and steady state operating conditions, the influence of external perturbations, the presence of model uncertainties.

Experiment N.2 (Test bench). The objective, here, is to illustrate the dynamic behavior of the speed controller as observed on the test bench. For this the vehicle is requested to follow a straight line in correspondence with a trapezoidal speed-time profile with a height equal to 1.2 m/s. The ensuing results (figure 8) show the vehicle speed response in the case where only the feedforward component of control action u_M is applied as compared to the case where both feedforward and feedback actions are applied. These figures also illustrate the influence of a perturbation equivalent to ξ_1=1 volt. These results confirm that the insertion of the feedback controller component offers a considerably better dynamic performance, a greater robustness to external perturbation, and a speed offset

dynamics relatively independent from the requested speed trajectory. The oscillations that one notices during the steady state part of the speed trajectory are due to the presence of elasticity in the belt linking the optical encoders to the drive wheels. They could be easily eliminated by simply improving such a linkage.

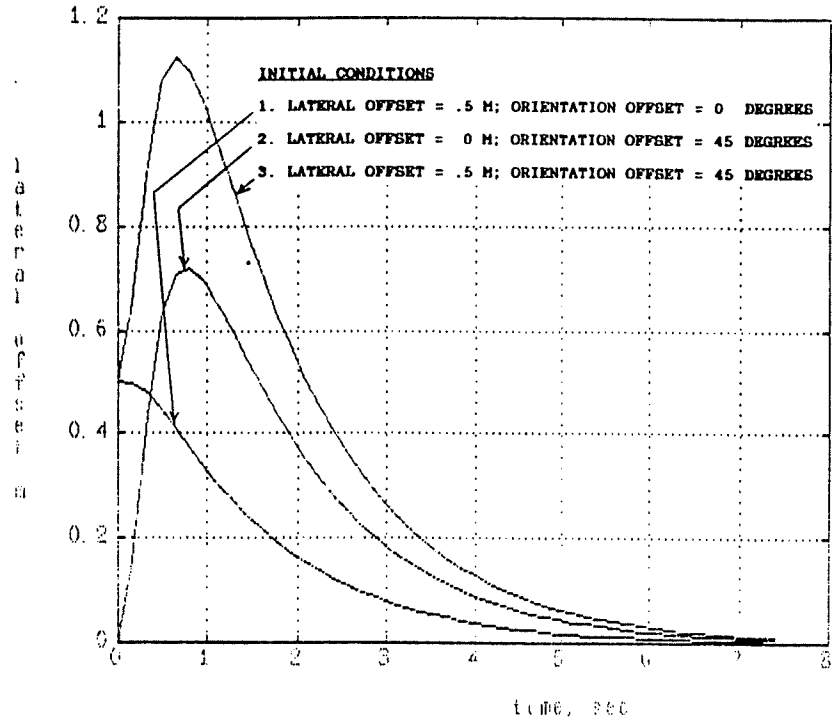

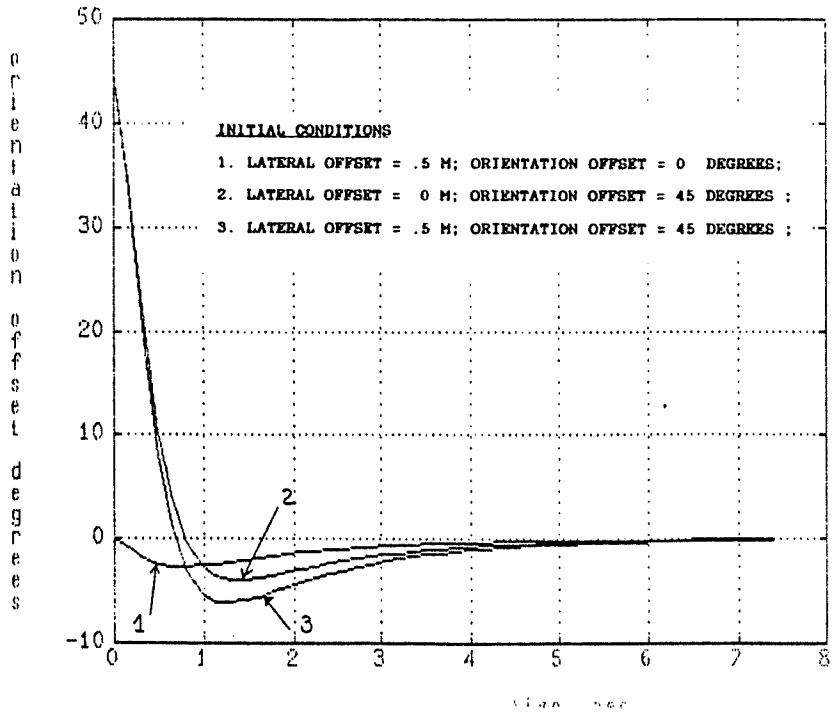

Figure 7: Position/orientation controller behavior (Exp 1, simulation results): i) lateral offset; ii) orientation offset

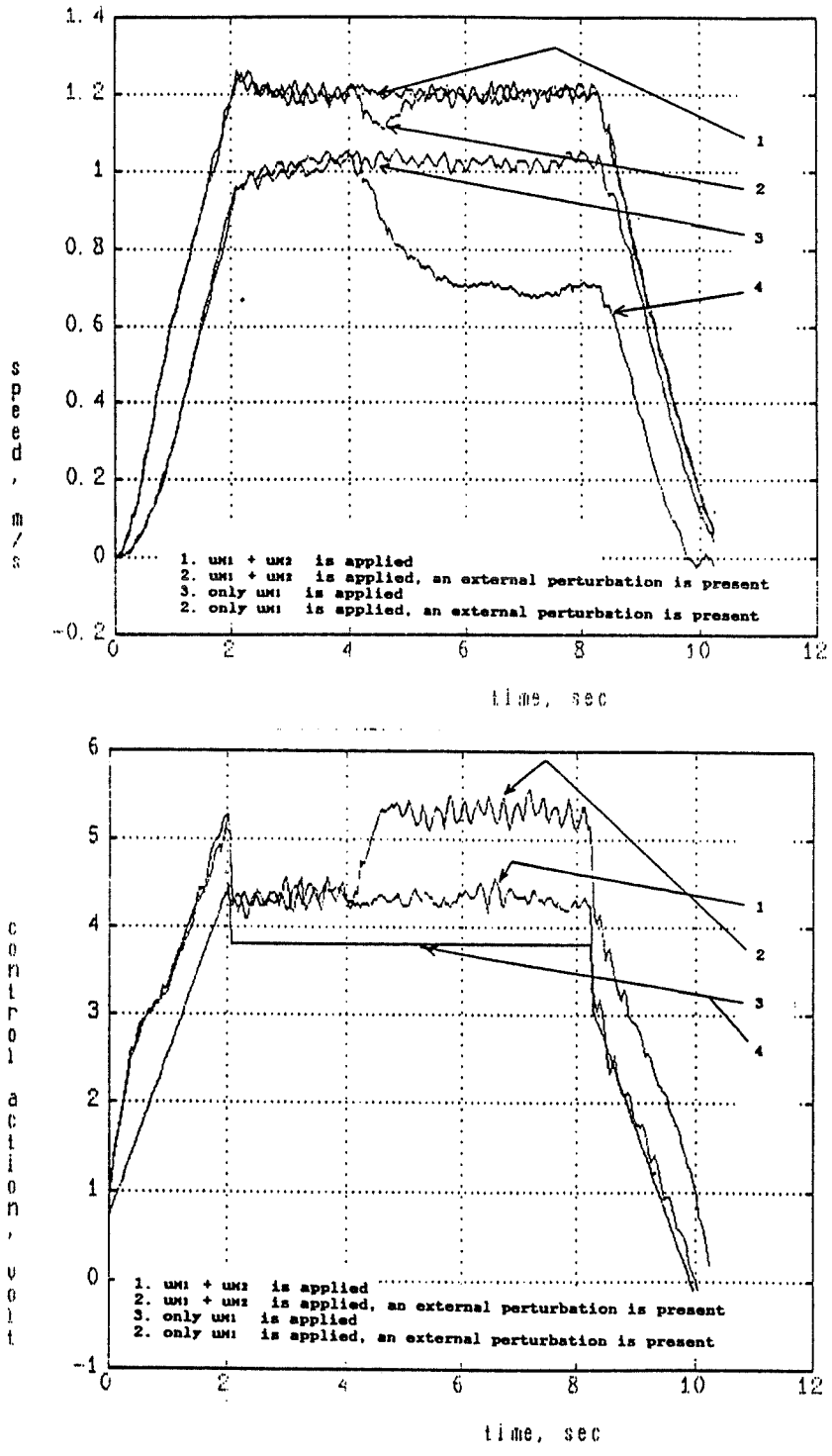

Figure 8: Speed controller behavior (Exp 2, field tests results): i) speed response; ii) control action

Experiment N.3 (Test bench). This experiment is set up to illustrate the dynamic behavior of the motion controller in relation with position and lateral offsets. The vehicle is now required to follow with a constant speed a path consisting of two straight line segments with a 15 degrees difference in orientation. Figure 9 shows the vehicle lateral and orientation offset responses. It can once again be easily verified by a direct analysis and by simulation that these results are well in agreement with the theoretical development. Note in particular that, in line with our position/orientation controller strategy, the dynamics of the orientation offset is essentially independent from the vehicle speed while the dynamics of the lateral offset is not. This strategy could be modified so as to have inverse occuring by making the poles p_{2i} directly proportional to the desired speed.

Experiment N.4 (Simulation). The objective, here, is to illustrate the potential benefit attainable with the incorporation of the sliding mode on-off switching component. For this we consider the following simulation conditions (because of data availability at the time of writing locomotion module parameters different from those used in the previous experiments are considered): a strong static friction in the drive wheels (with an input equivalent value of 100 Volt); initial values of speed, lateral offset and orientation offset respectively equal to 0, -.5 m, and - 15 degrees; a request that the vehicle follow a straight line path with a constant speed equal to 5m/s. Since a strong static friction on the forward motion is hypothesized, the

values of M_1 and ϵ_1 are selected as equal to M_1 = 100 volt ϵ_1 = 0.01 rad; $a_{11} = -1/p_{11}$ = 0.5 sec. Since no perturbation nor uncertainty in regard to steering is considered, the selected values of M_2 and ϵ_2 are equal to zero.

Figure 10 illustrates what happens on the dynamic behavior of the vehicle in the case where the linear speed controller is used (M_1 = 0). At the beginning of the experiment the static friction has a stronger value than the proportional control torque applied to the wheels: the vehicle remains then stuck until the integral control action becomes sufficiently strong to overcome the friction. Figure 11 shows that the same static friction has almost no influence on the vehicle dynamics when the original controller is modified into a PI/slm : the response of the system with or without the presence of friction is essentially the same and corresponds to that obtained in the case of the original controller under no friction.

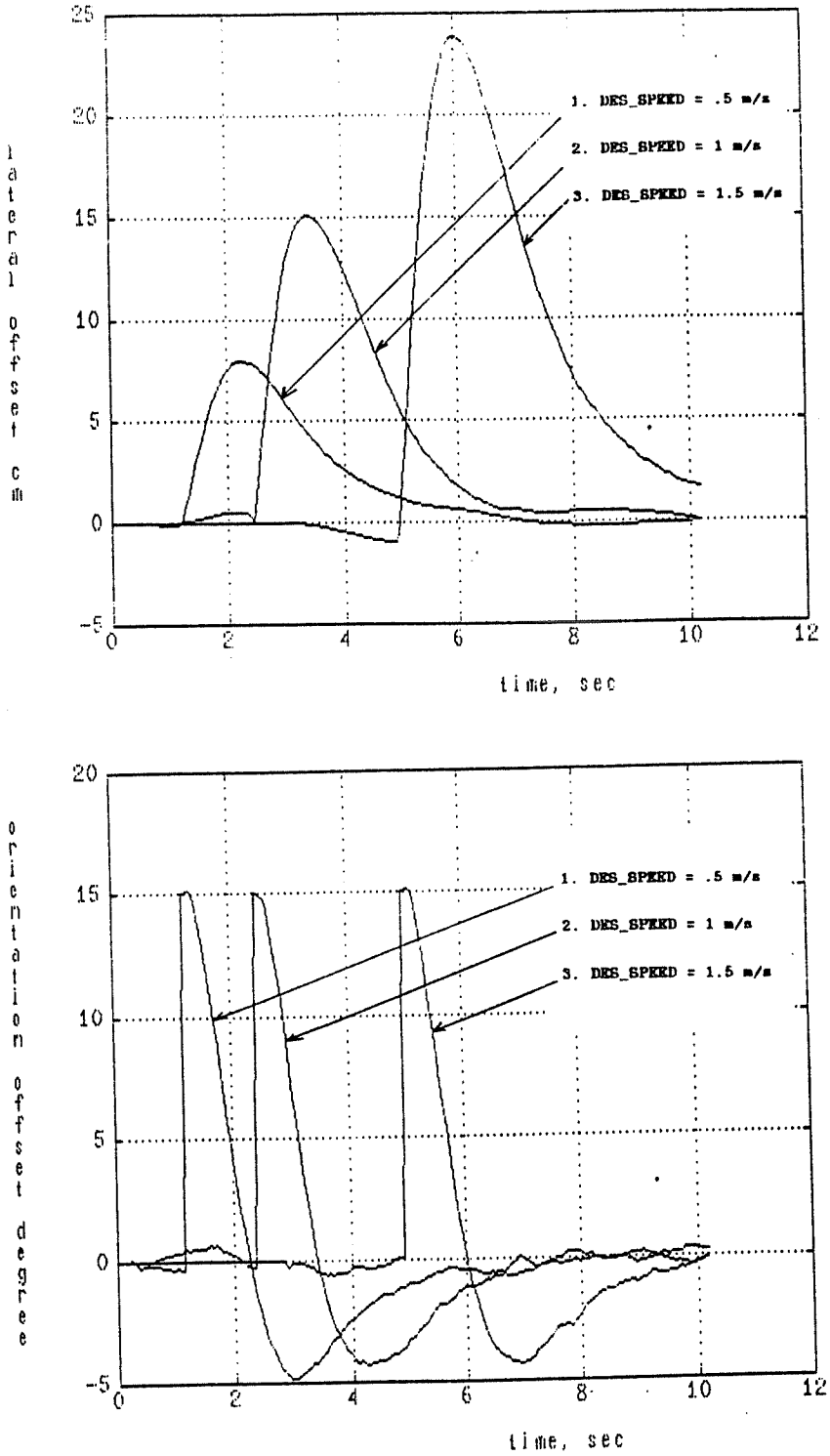

Figure 9: Position/orientation controller behavior (Exp 3, field tests results) i) lateral offset; ii) orientation offset

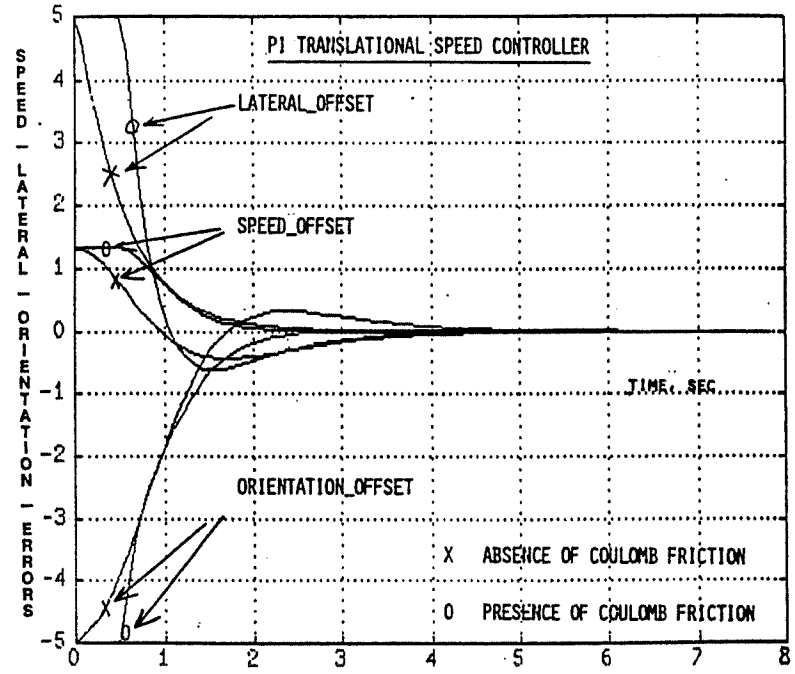

Figure 10: Effect of static friction in the classical PI speed controller (Exp 4, simulation results)

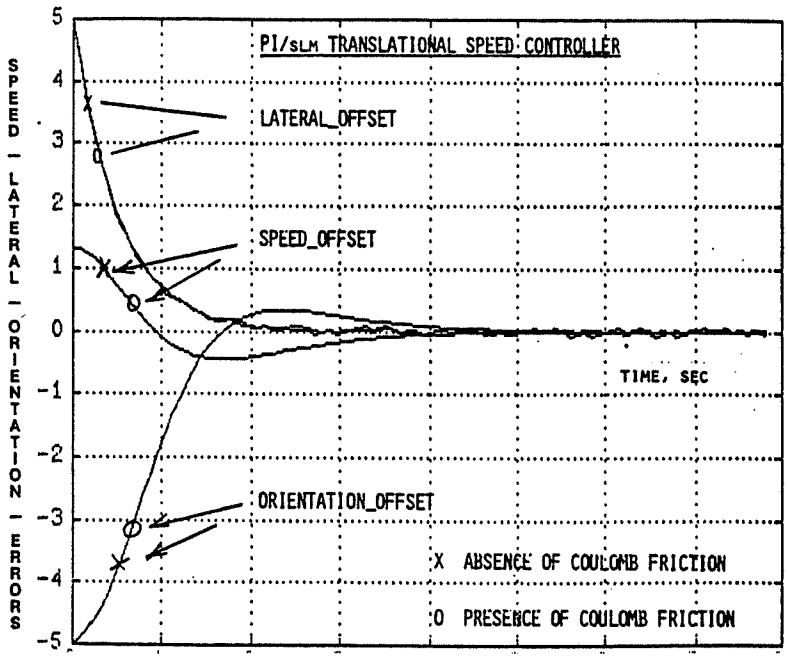

Figure 11: Effect of static friction in the PI/Slm speed controller (Exp 4, simulation results)

Conclusions

The proposed motion controller design procedure appears to be quite satisfactory and definetly adequate for the envisioned AGVs mining applications (and a large variety of others). It is simple and transparent; it is characterized by a good dynamic and static behavior; it is reasonably robust to model uncertainties and external perturbations; it leads to a good correspondence between theoretical and experimental behavior.

If required by particularly demanding circumstances, the proposed controller is easily amenable to incorporate more advanced features such as the inclusion of sliding modes, as we have discussed, or the insertion of auxiliary speed loops acting on each drive wheel, an integral correction of the lateral offset, the usage of adaptive control, learning and/or preview control and so on. For a definite evaluation of the practical benefits of these features, however, further test bench experiments would be required.

References

[1] Koivo, A.J., Fundamentals for Control of Robotic Manipulators. John Wiley & Sons Inc., 1989.

[2] Anderson, S.E, (Editor), Proceedings of the 3rd International Conference on Automated Guided Vehicle Systems, Stockholm, Sweden, October 1985.

[3] Hurteau, R., Piché, A., St-Amant, M., DeSantis, R.M., Development of an Autonomous Vehicle for Underground Mining Applications, DCIEM/RMC 2nd Workshop on Military Robotic Applications, RMC, Kingston, August 1989.

[4] Ellis, J.R., Vehicle Dynamics. London: London, Business Books, 1969.

[5] Nisouger, R.L., Wormley, D.N., Dynamic Performance of Automated Guideway Transit Vehicles with Dual-Axle Streering, IEEE Trans. on Vehicules Technology, vol. VT-28, no. 1, Feb 1979.

[6] Fenton, R.E., Selim, I., On the Optimal Design of an Automotive Lateral Controller, IEEE Trans. on Vehicile Technology, vol. 37, no. 2, May 1988.

[7] Blake, A., Zisserman, A., Visual Reconstruction, MIT Press, Cambridge, Massachussets, 1987.

[8] Yap, C.K., Algorithmic Motion Planning, in Algorithmic and Geometric Aspects of Robotics, LEA Publishers, 1987.

[9] Kuo, B.C., Automatic Control Systems. Prentice Hall, 1987

[10] De Santis, R.M., On PI and PID/Sliding Mode Controllers, Advances in Communication and Control, Springer Verlag, Dec 1989.

[11] De Santis, R.M., An Adaptive PI/Sliding Mode Controller for a Speed Drive, ASME Dynamic Systems, Measurement and Control, Sept 1989.

[12] Borenstein, J., Koren, Y, Motion Control Analysis of a Mobile Robot, ASME journal of Dynamic Systems, Measurement and Control, June 1987, Vol 109, pp 73-79.

[13] Tsumura, T., Fujiwara, N., Shirakawa, T., Hashimoto, M., An Experimental System for Automatic Guidance of a Robotic Vehicle Following the Route Stored in Memory, 11th International Symposium on Industrial Robots, Tokio, 1981, pp. 187-193.

[14] Anonimous, DC Motors Speed Controls Servo Systems, Engineering Handbook by Electro-Craft Corp., Pergamon Press, 1977.

[15] Rabemanantsoa, M., Analyse par voie de Simulation du Système d'Autopilotage d'un Robot Mobile, M. Sc. Thesis, École Polytechnique de Montréal, August 1989.

[16] Vignola, P.-L., Hurteau, R., Identification des Paramètres du Modèle d'un Robot Mobile, RTXX, École Polytechnique de Montréal, (to appear).

[17] Brady, M., Hollerbach, J.M., Johnson, T.L., Lozano-Perez, Mason, M.T., Robot Motion: planning and control, MIT press 1983

[18] Laumond, J-P., Simeon, T., Chatila, R., Giralt, G., Trajectory Planning and Motion Control for Mobile Robots, IUTAM/IFAC Symposium on Dynamics of Controlled Mechanical Systems, June 1988, Springer Verlag.
[19] Horn, B. K. P., Robot Vision, MIT Press 1987

Acknowledgement

Help in the implementation of the experimental tests was received from Pierre-Luc Vignola; in the development of the simulation software from Monjy Rabemanantsoa.